The hot flow behavior of Al-2wt.%Cu-1wt.%Mn alloy based on Gleebe-3800 hot compression simulation

JinLong Chen, Hengcheng Liao* and Heting Xu

School of Materials Science and Engineering, Southeast University, Jiangsu Key Laboratory for Advanced Metallic Materials, Nanjing 211189, China

**: Corresponding author, professor of Southeast University, hengchengliao@seu.edu.cn*

Abstract: Flow behavior of Al-2.0wt.%Cu-1.0wt.%Mn aluminum alloy was investigated by hot compressive test using a Gleebe-3800 thermal simulator. The test parameters about temperature and strain rate range from 573K to 773 K and from $0.01s^{-1}$ to $5s^{-1}$, respectively, and the true strain is up to 0.6. It can be seen that the peak flow stress increases with increasing the strain rate and decreases by deformation temperature. And the deformation activation energy of Al-2.0wt.%Cu-1.0wt.%Mn alloy is 183.02KJ/mol. A constitutive equation has been constructed to predict the hot deformation behavior, and correlate the peak flow stress predicted with strain rate and deformation temperature.

1. Introduction

Al-Cu-Mn series alloys have high strength at elevated temperature and high strength to weight ratio, so it has become a kind of prospective armor material to be used in chariot, aero-craft and other commercial machines. With the development of technology, the aircraft flight velocity is further increased, thus, further improvement of strength at elevated temperatures of aluminum alloy is needed.

Many plastic forming methods are used to further improve the strength and formability of aluminum alloys such as accumulative roll bonding(ARB), equal-channel angular pressing (ECAP)[1], cross-channel extrusion(CCE)[2], severe cold rolling, hot rolling[3], high pressure torsion(HPT) and so on in addition to the alloying. For examples, Vaseghi and Kim [4] obtained the high hardness of Al-Mg-Si alloy from 86 HV (as solution treatment) to 138 HV by ECAP. Chou et al.[5] reported that after solutionizing the tensile strength of Al-Mg-Si alloy was improved to 364 MPa by 8 passes of EACP at 448 K and then artificial aged, 13% higher than that in T6 state. Krishnaiah et al.[5] studied that the grain size of pure Al could be reduced from 38 μm to almost 1 μm by groove pressing. Jayaganthan et al. [3] investigated that the Al 6061 alloy by cryorolling followed by warm rolling can get a significant improvement in tensile strength (376MPa) and partial improvement in ductility (5%) as measured from tensile testing.

The peak flow stresses and the activation energy (Q) are measure indexes of difficulty for deformation. Deng et.al [6] studied the flow behaviors of tension and compression considering the influence of deformation temperature and strain of 2024 aluminum alloy. Bardi et.al [7] investigates the correlation between the flow stresses and dynamic precipitation of 2618 aluminum alloy by means of torsion tests at temperatures between 423 and 573 K. Li et.al [8] used a Gleeble-1500 machine to investigate the flow stress features of 2519A aluminum alloy and to determine the optimum hot-working condition. Li et.al [9] studied the hot deformation behaviors of Ag-containing 2519 aluminum alloy by isothermal compression at 300 ^{o}C-500 ^{o}C with strain rates from 0.01s^{-1} to 10s^{-1}. Liu et.al [10] studied the flow behavior of Al-Cu-Mg-Ag alloy and obtained the value of hot deformation activation energy of the alloy. Few researchers study the hot flow behaviors of Al-Cu-Mn alloys with low Cu content, and relation of the precipitation phase T_{Mn} to the flow behavior.

In this article, the hot deformation behavior of Al-2.0wt.%Cu-1.0wt.%Mn alloy is investigated at various temperatures and strain rates by Gleeble-3800 thermal simulator. The constitutive equation for the alloy is constructed relating flow stress, deformation temperature, strain rate, Zener–Hollomon parameter, and activation energy to deformation.

2. Experimental procedures

Al-2.0wt.%Cu-1.0wt.%Mn alloy was prepared in an electric resistance furnace using pure aluminum ingot and Al-20wt.%Cu and Al-10wt.%Mn master alloys. The chemical composition of the prepared alloy (Marked as A_1 alloy), measured by an MAX ×LMF15 spectrum, is listed in Table 1. After processing, the melts were poured into a metal mold with a size cavity size of 170mm×20mm×100mm (preheated at 250^{o}C for at least 5 hrs). Then small cylindrical specimens with 12 mm in height and 8 mm in diameter were cut from the castings, then solution-treated at 525 ^{o}C for 6 hrs +535 ^{o}C for 6hrs and terminated by a water quench.

A Gleebe-3800 thermal simulator is used to accomplish the isothermal compression test. In order to minimize friction and to make the specimen deform uniformly during the test, graphite foils were used as lubricant. Five temperatures (573, 623,673, 723 and 773 K) and four strain rates (10^{-2}, 0.1, 1 and 5 s^{-1}) were chosen as the experimental parameters. Specimens were heated to the test temperature at a heating rate of 5 K/s and held for 1.5 minutes. The specimens were compressed to a final strain of 0.6. The true strain–stress curves were recorded automatically. After deformation, the specimens were quenched immediately by water to preserve the as-deformed microstructure.

Table1 Chemical composition of the studied alloy (wt.%)

Alloy	Cu	Mn	Si	Fe	Al
A_1	2.04	0.998	0.064	0.131	Bal.

3. Results and discussion

3.1Flow stress characteristics

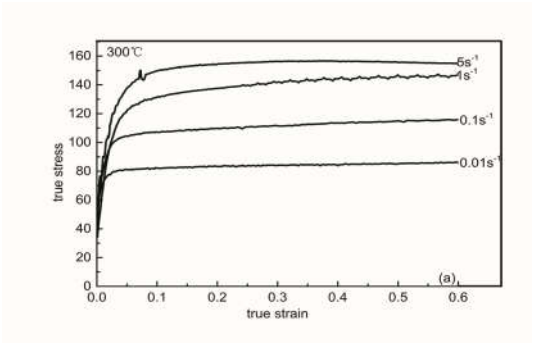

(a)

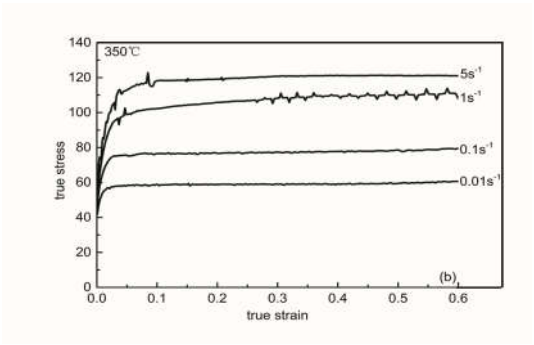

(b)

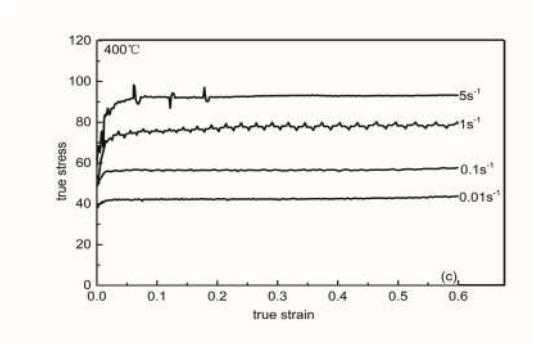

(c)

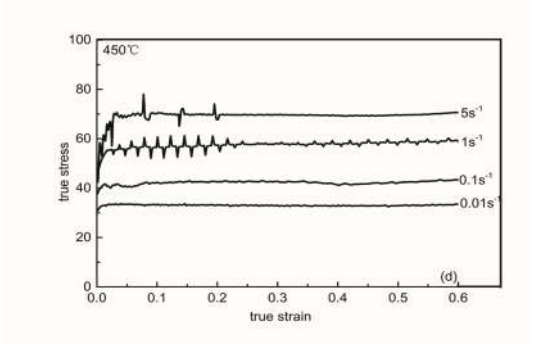

(d)

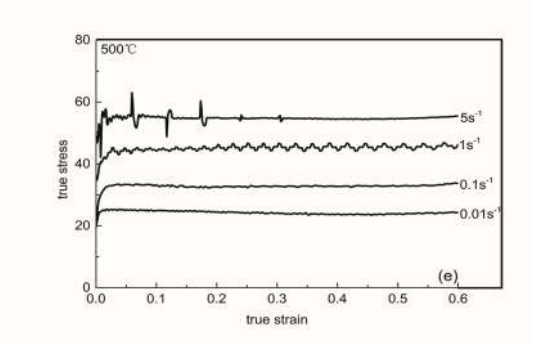

(e)

Fig.1 True stress–true strain curves of A_1 alloy obtained from hot compression tests at deformation temperatures of (a) 300 °C (b) 350 °C (c) 400 °C (d) 450 °C (e) 500 °C

The flow curves (σ vs ε) for Al-2.0wt.%Cu-1.0wt.%Mn alloy obtained at various strain rates ($\dot{\varepsilon}$) and deformation temperatures (T) are shown in Fig.1 through hot compressive tests. The stress values corresponding to the deformation temperature at 573K(300°C) and strain rate at $5s^{-1}$ are the highest, and the peak stress increases with increasing the strain rate for a given strain because there is not enough time to fully recrystallize in high strain rate, and decreases by deformation temperature due to the recovery or recrystallization. It is consistent with the results reported by Li et al.[11]and Ou et al.[12].

Fig.1 also shows that at 300 °C and 350°C with a high strain rate ($5s^{-1}$), the flow stress is increased considerably with strain when the material has just yields. This is due to the strain hardening caused by multiplication and interaction between dislocations and particles. With further increase in strain, the flow stress remains almost constant during the whole compression process, owing to the balance of strain hardening and softening from dynamic recovery or recrystallization. At the high deformation temperature above 350 °C and low strain rate of $0.1s^{-1}$ and $1s^{-1}$, the flow stress keeps constant after yielding. It is worth noting that at all the deformation temperatures with a strain rate of $1s^{-1}$, serrated wave lines exhibit, which may be the typical character of dynamic recrystallization. At the deformation temperature of 300 °C and 350 °C, the waves present only at the high strain, but at the higher deformation temperatures, waves pass through the plastic deformation stage. Especially at 450 °C, the

waves fluctuate violently first, and then become weakened.

3.2 Activation energy for deformation

It is usually accepted the flow behavior of material is controlled by thermal activation at elevated temperature, which is always described using Arrhenius type equation, in which a variable of activation energy is contained that stands for the difficulty for deformation.

The flow stress of hot deformation material depends on the deformation temperature, strain rate and true strain. When the true strain is fixed, the flow stress just depends on the deformation temperature and strain rate and several equations are used to relate the flow stress to strain rate,

$$\dot{\varepsilon} = A_1\sigma^{n_1}\exp(-\frac{Q}{RT}) \quad \text{when } \alpha\sigma<1.2 \tag{1}$$

$$\dot{\varepsilon} = A_2\exp(\beta\sigma)\exp(-\frac{Q}{RT}) \text{when} \alpha\sigma>1.2 \tag{2}$$

$$\dot{\varepsilon} = B[\sinh(\alpha\sigma)]^n\exp(-\frac{Q}{RT}) \text{ for all } \sigma \tag{3}$$

in which R is the universal gas constant (8.314 J mol^{-1} K^{-1}), T is the absolute temperature (K), Q is the activation energy of hot deformation(kJ.mol^{-1}). Moreover, A_1, $A2$, A, α, β, n_1, n are material constants, and $\alpha = \beta/n_1$.

The material constants in constitutive equations afore-mentioned are calculated through extracting the true stress-true strain data from the compression tests. Steady state true stress data at true strain of 0.3 are usually taken to evaluate the material constants above. For low and high stress levels, natural logarithm is taken at both sides of Eqs. (1) and (2), and then the following equations can be obtained:

$$\ln\dot{\varepsilon} = \ln A_1 + n_1\ln\sigma - \frac{Q}{RT} \tag{4}$$

$$\ln\dot{\varepsilon} = \ln A_2 + \beta\sigma - \frac{Q}{RT} \tag{5}$$

Then, the values of the flow stresses and the corresponding strain rates under the strain of 0.3 are substituted into Eqs. (4) and (5) , the data of σ, lnσ and ln$(\dot{\varepsilon})$ are computed, then plots ln$(\dot{\varepsilon})$-lnσ and ln$(\dot{\varepsilon})$-σ linearly according to the figures as shown in Fig 2. The average value of slopes are used to derive the values of n_1 and β , 8.267 and 0.132MPa^{-1}, respectively, so α=0.016MPa^{-1}.

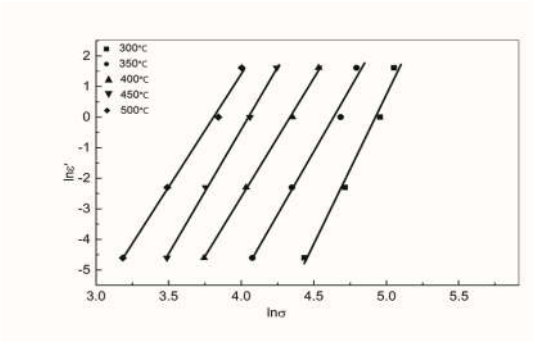

(a)

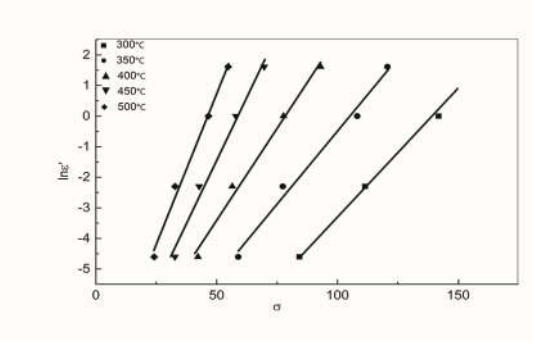

(b)

Fig.2 Relationship of (a) ln$(\dot{\varepsilon})$*vs* lnσ for alloy A_1, (b) ln$(\dot{\varepsilon})$ *vs* σ for the studied alloy during hot compression

Taking partial differential equation of Eq. (4) into consideration yields:

$$Q = R\left[\frac{\partial\ln\dot{\varepsilon}}{\partial\ln[\sinh(\alpha\sigma)]}\right]\left[\frac{\partial\ln[\sinh(\alpha\sigma)]}{\partial(1/T)}\right]_T = Rn_2s \tag{6}$$

The relationships of ln $\dot{\varepsilon}$ -ln[sinh$(\alpha\sigma)$] and ln[sinh$(\alpha\sigma)$]-$1/T$ are plotted in Fig.3. As a result, the value of n_2 and s are determined by calculating the average slope of two groups of lines. So n_2=5.88, s=3.744 and Q=183.02kJ/mol.

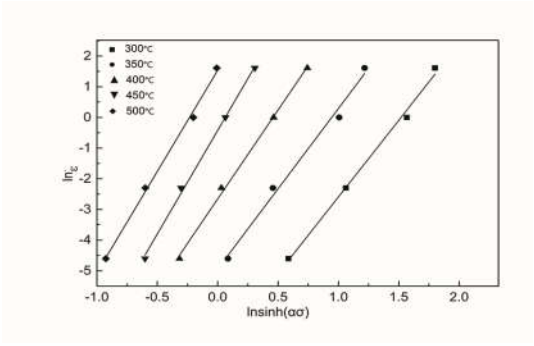

(a)

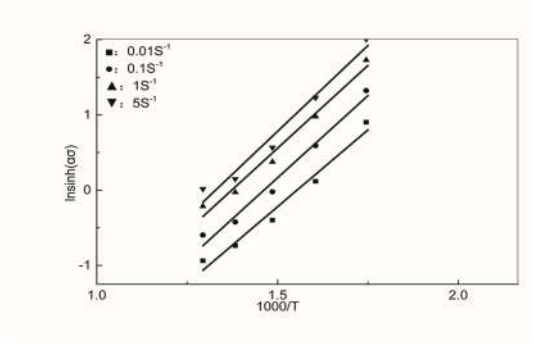

(b)

Fig.3 Relationship of (a) lnε-ln[sinh(ασ)] for the studied alloy (b) $\ln[\sinh(\alpha\sigma)]-1/T$ for A_1 alloy

3.3 Constitutive equations

The Zener-Hollomon parameter representing the temperature modified strain rate is used to illustrate the variation of flow stress with deformation conditions. The correlation between the Zener-Hollomon parameter with the strain rates, deformation temperature, and activation energy is expressed by the equation as follows:

$$Z=\dot{\varepsilon}\exp(\frac{Q}{RT}) \tag{7}$$

Combining Eqs.1-3 with (7), then, taking the logarithms, yields:

$$lnZ=\ln B+n\ln[\sinh(\alpha\sigma)] \tag{8}$$

Where B and n are derived from the ln*Z vs.* ln*[sinh(ασ)]* plots. By substituting the values of *Q* and different hot deformation conditions into Eq. (1), *Z* values are calculated subsequently. The values of ln*(Z)* for various strain rates and deformation temperatures can be evaluated for all the alloys studied. It is evident that *Z* increases with the increased strain rate and decreases by deformation temperature, which is similar to the variation of the peak flow stress *(σ)* shown in Figs.1. Liu et al. [13] reported that dynamic recrystallization is generally favored at low *Z* values, which corresponds to low strain rates and high deformation temperatures.

Then the relationship between ln*Z* and ln[sinh*(ασ)*] is shown in Fig.4. So we can derive the values of ln*B* and *n* are 30.03 and 6.65 for A_1 alloy, respectively.

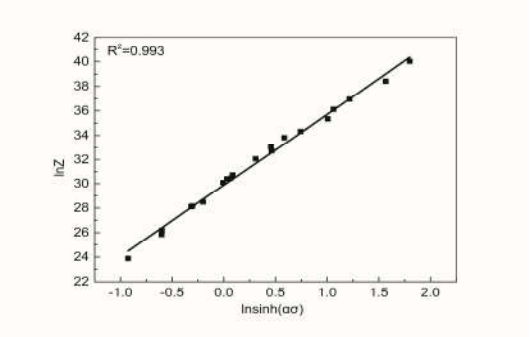

Fig.4 Plot of ln*Z* vs ln[sinh*(ασ)*] for Alloy-A_1

We can get the values of materials constants n_1, β, α, n_2, *Q*, ln*B* and *n* in constitutive equations of A_1 alloy at ε= 0.3 are 8.857, 0.107, 0.0122, 6.156, 222.84, 36.95 and 6.03, respectively. So the constitutive equation of the studied alloy (A_1) for ε=0.3 is given as following:

$$\dot{\varepsilon}=9.48\times10^{12}[\sinh(0.016\sigma)]^{5.88}\exp(-\frac{183020}{RT}) \tag{9}$$

4. Conclusions

Hot deformation behaviors of Al-2Cu-1Mn alloy were researched by isothermal compression using a Gleebe-3800 thermal simulator. The main results are summarized as follows:

(1)The deformation activation energy for Al-2Cu-1Mn alloy is obtained as 183.02KJ/mol through hot compressive test using a Gleebe-3800 thermal simulator.

(2)The constitutive equation for A_1 alloy has been established relating flow stress to deformation temperature and strain rate.

(3)It is easier to start dynamic recrystallization at higher temperature with strain rate $1s^{-1}$ than other conditions.

Acknowledgements

This work is supported by Jiangsu Key Laboratory Metallic Materials (Grant no. BM2007204) and the Fundamental Research Funds for the Central

Universities (Grant no.2242016k40011). The authors are also thankful to Sha-steel Iron and Steel Research Institute of Jiangsu Province for their useful assistance.

References

[1]S. Nicolae, C. Vasile-Danut, B. Mihai, JOM. **64**, 607-614 (2012).

[2]C.Y. Chou, C.W. Hsu, S.L.Lee, K.W.Wang, J.C.Lin, J.Mater. Process.Technol. **202**, 1-6 (2008).

[3]P.Nageswara Rao, R.Jayaganthan, Mater. Des.**39**, 226-233 (2012).

[4]M.Vaseghi, H.S. Kim, Mater. Des. **36**, 735-740 (2012).

[5]A.Krishnaiah, U.Chakkingal, P. Venugopal, Scripta Mater. **52**, 1229-1233 (2005).

[6] L. Deng, T. Zhao, J.S. Jin, X.Y. Wang, 11th International Conference on Technology of Plasticity, ICTP 2014, 19-24 October 2014,Nagoya Congress Center, Nagoya, Japan.

[7]F. Bardi, M. Cabibbo, S. Spigarelli, Mater.Sci.Eng.A **334**, 87-95 (2002).

[8]H.Z. Li, H.J. Wang, X.P. Liang, H.T. Liu, Y. Liu, X.M. Zhang, Mater.Sci.Eng.A **528**, 1548-1552 (2011).

[9]H.Z. Li, Z. Li, M. Song, X.P. Liang, F.F. Guo, Mater.Des.**31**, 2171-2176 (2010).

[10]X.Y. Liu, Q.L. Pan, Y.B. He, W.B. Li, W.J. Liang, Z.M. Yin, Mater.Sci.Eng.A **500**, 150-154(2009)**.**

[11]B.L, Q.L.Pan, Z.Y.Zhang, J Mater Eng Perform. **22**, 536-540 (2013).

[12]L.Ou, Y.F.Nie, Z.Q.Zheng, J Mater Eng Perform. **23**, 25-30 (2014).

[13]X.Y. Liu, Q.L. Pan, Y.B. He, W.B. Li, W.J. Liang, Z.M. Yin, Mater.Sci.Eng.A **500**, 150-154 (2009).